

# Young Stellar Populations Around SN 1987A<sup>†</sup>

Nino Panagia<sup>1</sup>

Space Telescope Science Institute, 3700 San Martin Drive, Baltimore, MD 21218

Martino Romaniello

ESO, Karl-Schwarzschild-Straße 2, D-85748 Garching bei München, Germany

Salvatore Scuderi

Osservatorio Astrofisico di Catania, Viale A. Doria 6, I-95125, Catania, Italy

and

Robert P. Kirshner

Harvard-Smithsonian Center for Astrophysics, 60 Garden Street, Cambridge, MA 02138

Received \_\_\_\_\_; accepted \_\_\_\_\_

submitted to the Ap.J.

---

<sup>†</sup>Based on observations with the NASA/ESA Hubble Space Telescope, obtained at the Space Telescope Science Institute, which is operated by AURA, Inc., under NASA contract NAS 5-26555.

<sup>1</sup>On assignment from the Astrophysics Division, Space Science Department of ESA

## ABSTRACT

We present the first results of a study of the stellar population in a region of 30 pc radius around SN 1987A, based on an analysis of multi-band *HST-WFPC2* images.

The effective temperature, radius and, possibly, reddening of each star were determined by fitting the measured broad band magnitudes to the ones calculated with model atmospheres. In particular, we have determined effective temperatures and bolometric luminosities for 21,995 stars, and for a sub-sample of 2,510 stars we also determined individual reddening corrections. In addition, we have identified all stars with  $\text{H}\alpha$  equivalent widths in excess of 8 Å amounting to a total of 492 stars.

An inspection to the HR diagram reveals the presence of several generations of young stars, with ages between 1 and 150 *Myrs*, superposed on a much older field population (0.6 – 6 *Gyrs*). A substantial fraction of young stars have ages around 12 *Myrs* which is the stellar generation coeval to SN 1987A progenitor. The youngest stars in the field appear to be strong-line *T Tauri* stars, identified on the basis of their conspicuous ( $W_{eq} > 8\text{\AA}$ )  $\text{H}\alpha$  excesses. This constitute the first positive detection of low mass (about 1-2  $M_\odot$ ) Pre-Main-Sequence (PMS) stars outside the Milky Way. Their positions in the HR diagram appear to require that star formation in the LMC occurs with accretion rates about 10 times higher than in the Milky Way, *i.e.*  $\sim 10^{-4} M_\odot \text{ yr}^{-1}$ .

SN 1987A appears to belong to a loose, young cluster  $12 \pm 2$  Myrs old, in which the slope of the present mass function is almost identical to Salpeter's, *i.e.*  $\Gamma = d\log N/d\log M \simeq -1.25$  for masses above  $3 M_\odot$ , but becomes much flatter for lower masses, *i.e.*  $\Gamma \simeq -0.5$ .

On a large scale, we find that the spatial distribution of massive stars and

low-mass PMS stars are conclusively different, indicating that different star formation processes operate for high and low mass stars. This results casts doubts on the validity of an Initial Mass Function (IMF) concept on a small scale (say, less than  $10pc$ ). Moreover, it appears that a determination of the low-mass end IMF in the LMC requires an explicit identification of PMS stars. A preliminary analysis, done for the whole field as a single entity, shows that the IMF slope for the young population present over the entire region is steeper than  $\Gamma \simeq -1.7$ .

*Subject headings:* (stars:) supernovae: individual (SN 1987A), galaxies: individual (LMC), stars: early-type, stars: pre-main sequence, stars: evolution

## 1. Introduction

SN 1987A has been one of the first targets ever observed with *HST*. It was first imaged with the FOC on August 23-24 1990, immediately revealing the high potential of *HST* observations, despite the unfortunate problem of spherical aberration, with an impressive display of the supernova itself, flanked by its companion stars, Star 2 and 3, and the famous inner circumstellar ring (Jakobsen et al. 1991, Panagia et al. 1991). The full *HST* capabilities were reached only after the first refurbishment mission in December 1993. And surely enough, SN 1987A caught everybody's eye with its beautiful triple ring circumstellar nebula which was imaged with the new *WFPC2* (Burrows et al. 1995, Panagia et al. 1996). Since then, SN 1987A has regularly been imaged in a number of broad and narrow band filters at least once a year as part of the SINS (Supernova INtensive Study, PI: Kirshner) project to monitor the evolution of the supernova as well as the changes in the emission of the rings. The combination of these images, always centered on the supernova but taken with different roll angles, resulted in an excellent coverage of an area of about  $130''$  radius, *i.e.* about 30 pc, around SN 1987A.

SN 1987A is located about 20 arcminutes SW of the edge of the 30 Doradus nebula. This area includes regions of very active star formation, in which different groups of early type stars are interspersed with HII regions and SNR shells. The association closest to SN 1987A is LH 90, which is located about 5 arcminutes to the NE of the supernova (Lucke and Hodge 1970) and whose age is much younger than that of SN 1987A progenitor, *i.e.* about 4 *Myrs* as compared with the 10-11 *Myrs* as estimated for Sk -69 202 (*e.g.* Van Dyk et al. 1998). The supernova itself is surrounded by a number of bright blue stars that seem to cluster around it. It is clear that the study of SN 1987A neighborhood offers a unique opportunity to place the supernova explosion in the proper context of stellar evolution and the evolution of stellar populations.

Here, we present the first results of a systematic study of the stellar populations contained in a field of  $130''$  radius (*i.e.* about  $30\text{ pc}$ ) around SN 1987A, focusing mostly on the properties of the younger populations. We show that several distinct generations of young stars can be identified in addition to the one that gave birth to the SN progenitor, with ages spanning from  $1\text{ Myr}$  or less to at least  $100\text{-}150\text{ Myrs}$ . Thanks to  $\text{H}\alpha$  narrow band photometry, we have identified almost 500 strong-line T Tauri stars: this constitutes the first positive (spectroscopic) detection of moderate/low mass (about  $1\text{-}2\text{ }M_\odot$ ) Pre-Main-Sequence (PMS) stars outside the Milky Way <sup>2</sup>. Their detection provides an excellent tracing of the spatial distribution of low mass PMS stars which is compared with the one of coeval, more massive stars. On this basis, we show that within the stellar generation of SN 1987A the more massive stars ( $M > 6\text{ }M_\odot$ ) are mostly grouped around the SN progenitor whereas lower mass stars ( $1M_\odot < M < 2\text{ }M_\odot$ ) are more evenly distributed, suggesting that different formation mechanisms are operating for stars of different masses. Finally, we consider and discuss the problem of determining the Initial Mass Function (IMF), concluding that an explicit identification of pre-MS stars based on spectroscopic criteria is absolutely necessary to separate young, low-mass stars from older population, field stars properly.

## 2. Observations and Data Reduction

Since 1994, Supernova 1987A was imaged with the *WFPC2* every year as a part of the SINS project. The log of the observations we have used is reported in Table 1. We did not use the observations of March 3, 1995, since only 4 bands were taken and they did not

---

<sup>2</sup>Existing studies of other young regions (*e.g.* Gilmozzi *et al.* 1994, Hunter *et al.* 1995) in the LMC have already found PMS stars but only in a statistical sense, *i.e.* identifying them only on the basis of their location in the HR diagram.

provide any significant addition to the portion of sky covered by the other ones. Among all SINS images taken until 1997, only for one epoch (July 1997) was the field observed in the  $\text{H}\alpha$  filter. Since, as shown in Sections 4 and 5,  $\text{H}\alpha$  images are essential in studying the young population, we complemented the SINS data with the  $\text{H}\alpha$  images taken for *HST* program #5203 (PI: John Trauger) on February 3, 1994, which overlap almost exactly with the SINS images obtained in February 1996 with broad band filters.

EDITOR: PLACE TABLE 1 HERE

The observations were processed through the standard PODPS (Post Observation Data Processing System) pipeline for bias removal and flat fielding. In all the cases the available images for each filter were combined to remove cosmic rays events.

The plate scale of the camera is 0.045 and 0.099 arcsec/pixel in the PC and in the three WF chips, respectively. We performed aperture photometry following the prescriptions by Gilmozzi (1990) as refined by Romaniello (1998), *i.e.* measuring the flux in a circular aperture of 2 pixels radius and the sky background value in an annulus of internal radius 3 pixels and width 2 pixels. Aperture photometry is perfectly adequate for our study because crowding is never a problem in our images. Actually, the average separation of stars from each other is about  $1.3''$  (*i.e.*  $\sim 29$  pixels in the PC chip and  $\sim 13$  pixels in the WF one) which is much larger than the *WFPC2* PSF width. The flux calibration is obtained using the internal calibration of the *WFPC2* (Whitmore 1995), which is typically accurate to within  $\pm 5\%$ . We use the spectrum of Vega as photometric zero point. However, since we have used the *IRAF-synphot* synthetic photometry package to compute the theoretical Data Numbers to be compared to the observed ones, the choice of the zero points has no influence on the final results.

The brightest stars in each CCD chip are saturated (*i.e.* most stars brighter than 17.5

in the F555W band). We recover their photometry either by fitting the unsaturated wings of the PSF for moderately saturated stars, *i.e.* with no saturation outside the central 2 pixel radius, or by following the method developed by Gilliland (1994) for heavily saturated stars. In most cases, the achieved photometric accuracy is better than 0.05 magnitudes. Full description of the methods used can be found in Romaniello (1998) and Romaniello *et al.* (1999b). As a sanity check we have compared our photometry in the B and V bands with the one obtained with ground based observations (28 stars brighter than  $V \simeq 20$  within  $30''$  from SN 1987A; Walker and Suntzeff 1990) and found an overall excellent agreement, *i.e.*  $rms$  deviations less than 0.05 *mag* in both bands, except for the obvious cases of few stars that appear as point-like objects in ground based images but are resolved by *HST* observations.

Figure 1 shows the entire field as observed in a mosaic of B, V, and R broad band plus the [OIII] and H $\alpha$  narrow band images. As mentioned in the introduction, SN 1987A appears to be part of a group of early type stars, whose spatial density is significantly higher in the neighborhood of the supernova than in the remaining area, suggesting the presence of a physical group and/or a small cluster. Quantitatively, the number of stars brighter than  $B = 18$  *mag* in the inner  $20''$  radius region (15 stars) is about 23% of the total 64 such stars contained within  $130''$  radius field, although the former has an area of only 4% of the total field.

EDITOR: PLACE FIGURE 1 HERE.

We identify the stars in the F555W exposure and then measure their magnitudes in all of the other filters. The total number of stars detected in this way is 21,955. For about 12,340 of them the photometric accuracy is better than 0.1 *mag* in the V, R and I filters. The number of stars with accuracy better than 0.1 *mag* drops to 6825 in the B band, and

only 786 stars have a UV filter uncertainty smaller than 0.2 *mag*.

### 3. Color-Magnitude Diagrams and HR Diagrams

Figure 2 displays the Color-Magnitude Diagrams (CMD) for four combinations of bands. In order to select stars with overall good photometry, we have used the average error in 5 bands ( $\bar{\delta}_5$ ), excluding the UV:

$$\bar{\delta}_5 = \sqrt{\frac{\delta_{F336W}^2 + \delta_{F439W}^2 + \delta_{F555W}^2 + \delta_{F675W}^2 + \delta_{F814W}^2}{5}} \quad (1)$$

EDITOR: PLACE FIGURE 2 HERE.

The black dots in each CMD in Figure 2 are the 5,979 stars with  $\bar{\delta}_5 < 0.1$  *mag*. The error threshold of  $\bar{\delta}_5 < 0.1$  reflects itself as a magnitude threshold at  $m_{F555W} \simeq 23$ . We estimate that completeness at this magnitude limit is very close to 100% because the density of detected stars down to 23th magnitude is rather low, *i.e.* about 1 star per 4.6 square-arcsec area. Thus, conservatively adopting an effective PSF area of 0.28 square-arcsec (*i.e.* a 3 WF-pixel radius circular area) and defining  $f$  as the probability of having one star brighter than 23rd magnitude falling in any one PSF area ( $f = 0.28/4.6 = 0.061$ ), a simple application of Poisson statistics predicts that only a fraction of  $[1 - fe^{-f}/(1 - e^{-f})] = 0.031$  of the stars may overlap with other stars.

It is apparent that, despite the high quality of the measurements (internal uncertainties less than 0.1 magnitudes), the various features of the CMDs, such as the Zero Age Main Sequence (ZAMS) and the sequence of binaries for the early type stars, and the red giant clump for the more evolved populations, are rather “fuzzy” and not sharply defined. Although this is due in part to the presence of several stellar populations projected on each

other (see Sections 4-6), most of the problem arises from the fact that reddening is not quite uniform over the field, thus causing the points of otherwise identical stars to fall in appreciably different locations of the CMDs.

The large number of bands available (6 broad band filters) which cover a wide baseline (more than a factor of 4 in wavelength, extending from  $\sim 2,300$  to  $\sim 9,600$  Å) provide us with a sort of *wide-band spectroscopy* which defines the continuum spectral emission distribution of each star quite well. Therefore, by comparison with model atmospheres (Bessel *et al.* 1998), one can fit the 6 band observations of each stars and solve for 3 unknowns simultaneously, namely the effective temperature,  $T_{eff}$ , the reddening,  $E(B - V)$ , and the angular radius,  $R/D$ . As well known, the solution in the plane  $T_{eff} - E(B - V)$  may not be unique for stars with effective temperatures lower than about 9,000 K. Therefore, we first solve for the full set of parameters,  $T_{eff}$ ,  $E(B - V)$ , and  $R/D$  only for stars suitably selected on the basis of reddening-free colors. These turn out to have temperature either higher than 10,000 K or between 6,750 and 8,500 K. For each of the remaining stars, we adopt the average reddening of its neighbors and solve for only two parameters,  $T_{eff}$ , and  $R/D$ . Finally the stellar luminosity is computed from the derived  $T_{eff}$  and  $R/D$  values, adopting a distance to SN 1987A of 51.4 kpc (Panagia 1999, Panagia *et al.* 1999, Romaniello *et al.* 1999b). A full account of this analysis will be presented in a forthcoming paper (Romaniello *et al.* 1999a; see also Romaniello 1998). Out of the total sample of 21,995 stars, the uncertainty in the effective temperature is lower than 12% for 9,474 stars, most of which with  $\log(L/L_\odot) > 0$ . Also, we were able to obtain individual reddening determinations for 2,510 stars (*i.e.* about 11% of the whole sample). On average, this corresponds to a reddening value every 13 square arcseconds, which implies that the extinction distribution over the entire field was mapped down to a scale size of about 3.5" (*i.e.* about 1 pc).

The reddening is clearly not constant over the field, having an average value of  $\langle E(B - V) \rangle = 0.203$  and a *rms* deviation  $\sigma(E(B - V)) = 0.072$ . The average value is very close to the reddening determined by Scuderi *et al.* (1996) in the direction of Star 2 ( $0.19 \pm 0.02$ ) and by Walborn *et al.* (1993) from an analysis of photometric ground based observations of early type stars in the same field. The reddening spatial distribution does not correlate well with the distribution of nebular emission. Moreover, the reddening fluctuations do not show any obvious pattern, suggesting the presence of a highly clumped diffuse medium (*c.f.* Romaniello 1998, Romaniello *et al.* 1999a).

#### 4. Stellar Populations and Ages

The resulting HR diagram ( $\log(L/L_\odot)$  *vs.*  $\log(T_{eff})$  plot) is shown in Figure 3. Its inspection confirms the early findings of Walker and Suntzeff (1990) and Walborn *et al.* (1993) and reveals that the distribution of stars in the HR diagram is clearly bound toward high temperatures, identifying a ZAMS that corresponds to a metallicity  $Z \simeq Z_\odot/3$  (*c.f.* Figure 3a). This value agrees well with the general abundances measured in the LMC as well as the more local estimates derived from spectroscopy of the circumstellar rings (Panagia *et al.* 1996) and Star 2 (Scuderi *et al.* 1996). Therefore, in the following the observed points will be compared with  $Z = 0.006$  isochrones, either from Brocato & Castellani (1993) and Cassisi, Castellani & Straniero (1994) for post-MS evolution or from Siess *et al* (1997) for PMS evolution.

EDITOR: PLACE FIGURE 3 HERE.

With the exception of one very bright star<sup>3</sup> (readily recognizable in Figure 1 and denoted with a larger symbol in Figures 3b and 6c), the positions of the most luminous blue stars (see Figure 3b) fall on isochrones corresponding to ages around 10-14 *Myrs*, which make them coeval to SN 1987A progenitor and Star 2 (*c.f.* Scuderi *et al.* 1996 and references therein). There are a number of stars at intermediate luminosities and temperatures that indicate ages up to 100-150 *Myrs* and initial masses down to  $4 M_{\odot}$ . This is especially clear from the position of the yellow/red supergiants around  $\log(T_{eff}) \sim 3.6 - 3.8$  and  $\log(L/L_{\odot}) \sim 2 - 3$ .

The lower MS and the Red Giants are mostly old population stars, consistent with a metallicity either identical to, or slightly lower than the one of the young components. No single age can explain the distribution of the old population, and substantial star formation between 600 *Myrs* and 6 *Gyrs* is required to account for the observations (*c.f.* Figure 3b).

In summary, we find evidence for a series of star formation episodes spanning from several billion years ago until at least 1-2 *Myrs* and, possibly, still ongoing (*c.f.* Figure 4 and Section 5). We identify a generation of stars with ages about 12 *Myrs* which is coeval to the supernova progenitor and may include up to 35% of the young population in this field (defined as stars with ages  $< 100$  *Myrs*). The old field population requires continued star formation over a broad interval of 0.6 – 6 *Gyrs*. From all of these results, it is clear that, since even the young stars belong to a mixture of populations of different ages, a study of the IMF is very hard and requires a proper separation of the various stellar generations to avoid systematic biases and errors.

---

<sup>3</sup>This star has  $\log(T_{eff}) = 4.7$ ,  $\log(L/L_{\odot}) = 5.8$ , which correspond to a mass of  $\sim 60 M_{\odot}$  and suggest an age probably younger than a million years.

## 5. Pre-Main-Sequence Stars and the Young Population

By comparing the magnitudes in the R band (F675W) with the ones measured with the narrow band H $\alpha$  filter (F656N) we can identify stars with sufficiently strong H $\alpha$  emission. Considering the throughputs of the F675W and F656N filters (*c.f. WFPC2 Instrument Handbook*, Biretta 1996) we estimate that an H $\alpha$  emission line with equivalent width of 8 Å will produce a color excess  $m(R) - m(H\alpha) \simeq 0.3$  mag. Therefore, we define as stars with strong H $\alpha$  excess the ones with a color excess  $m(R) - m(H\alpha)$  which is both greater than 0.3 and greater than 4 times the photometric uncertainty, *i.e.*  $> 4\sqrt{\sigma^2(R) + \sigma^2(H\alpha)}$ . The requirement on the error assures that a measured excess is highly significant, and the high equivalent width cutoff excludes any contamination by normal stars with chromospheric activity, because they have equivalent widths of less than 3 Å (*e.g.* Frasca and Catalano 1994). The positions in the HR of H $\alpha$  excess stars are shown in Figure 4 and compared with the distribution of all other stars.

EDITOR: PLACE FIGURE 4 HERE.

We identify the luminous and bright ones (4 stars), which are near the MS, as Be stars. One of them is Star 3, one of the two companions to SN 1987A (see Walborn et al. 1993 and references therein): its high variability qualifies it for a “typical” Be star (*c.f.* Jaschek et al. 1980). However, its emission lines are too narrow (*c.f.* Walborn et al. 1993) to conform to the characteristics of canonical Be stars. A possible explanation is that Star 3 is seen almost pole-on. On the other hand, we cannot exclude that Star 3 belongs to the same class of HAeBe stars, *i.e.* massive PMS stars (Herbig 1960), as the six possible candidates found near the center of the LMC bar by Lamers, Beaulieu and De Wit (1999). They concluded that the location in the HR diagram of their candidate HAeBe stars indicate a prevailing accretion rate of about  $10^{-4} M_\odot \text{ yr}^{-1}$ , *i.e.* ten times higher than the “canonical value” of

$10^{-5} M_{\odot} \text{ yr}^{-1}$  as appropriate for the Milky Way (*c.f.* Palla & Stahler 1993). Also our 4 Be stars, if they are considered to be stars evolving toward the Main Sequence, would require a considerably brighter birthline for the LMC than it is found for Milky Way stars (see Fig 4), again indicating accretion rates up to  $10^{-4} M_{\odot} \text{ yr}^{-1}$ . If the PMS nature of such stars is confirmed by detailed spectroscopic studies, these results would imply that star formation in a low metallicity environment proceed at a substantial different pace than it does in our Galaxies, at least for massive stars.

EDITOR: PLACE FIGURE 5 HERE.

We identify the redder and fainter stars with strong H $\alpha$  excess (488 stars, 275 of which have very accurate temperature determinations,  $\delta \log T_{\text{eff}} < 0.05$ ) as strong-line T Tauri stars, *i.e.* PMS stars with circumstellar material, remnant of their proto-stellar cocoons<sup>4</sup>. Their H $\alpha$  excesses correspond to H $\alpha$  equivalent widths which range between 8 and 360 Å, with 90% of the  $W_{\text{eq}}(\text{H}\alpha)$  values falling within 11 and 85 Å. These properties are very similar to the ones of galactic strong-line T Tau stars (*e.g.* Herbig & Bell 1988 Fernandez *et al.* 1995) although we note that the H $\alpha$  equivalent width distribution of T Tau stars in our field is more skewed toward lower values than the galactic ones (*c.f.* Fig. 5). This difference is easily explained as an age effect, in that classical galactic T Tau stars are much younger (ages below 5 Myrs) than the ones in our field. Comparing the positions of T Tauri stars in

---

<sup>4</sup>Confirmation of the reality of the measured H $\alpha$  excesses and the T Tau identification is provided by both a visual inspection to the images, which excludes the presence of nebular filamentary structures crossing each candidate star image, that may mimic an apparent “excess”, and measurements of the stellar fluxes in the [OIII] and [NII] narrow band filters (F502N and F658N, respectively) that for all of the *bona fide* T Tau candidate stars give line emission that are appropriately much lower than the emission measured for the H $\alpha$  line.

the HR diagram with PMS evolution model calculations by Siess *et al.* (1997), we find that most of them have masses in the range  $1-2M_{\odot}$  and ages between 1-2 *Myrs* up to 20 *Myrs* and possibly beyond (see Figure 4). Note that the presence of T Tau stars on, or very close to the birthline even suggests that some star formation is still ongoing in this field. Overall, T Tau stars represent about 4% of the total number of stars present in the same area of the HR diagram (approximately,  $\log(T_{eff}) = 3.65 - 3.95$  and  $\log(L/L_{\odot}) < 1$ ), making them very hard to identify without positive spectroscopic diagnostics.

We like to stress that this result constitutes the first positive detection of moderate/low mass (about  $1-2 M_{\odot}$ ) PMS stars outside the Milky Way. In fact, although previous studies of other young regions of the LMC (*e.g.* NGC 1850 by Gilmozzi *et al.* 1994, R136 cluster by Hunter *et al.* 1995, *etc.*) have already identified low mass “PMS stars”, those identifications were entirely circumstantial in that they were based exclusively on the location of the candidate stars in the HR diagram. In the following we will show that, because of heavy contamination by older, field populations of low mass stars, such an “identification” method may, at best, have just a statistical value and may lead to an overestimate of the actual number of low mass stars in a star forming region.

In Figure 6a and 6b we display the spatial distribution of massive stars, *i.e.* stars with  $M > 6 M_{\odot}$ , and strong T Tauri stars as defined above, overlaid on a mosaic of the  $H\alpha$  images. We see that massive stars are strongly concentrated near SN 1987A (14 out of 55 are within 20'' of the supernova), and the remaining ones are mostly located East of SN 1987A (31 out of 41). The PMS stars, on the other hand, do not show any strong spatial concentration, although one can notice that the number density of PMS stars on the NE side of SN 1987A is appreciably lower than on the SW side. No obvious correlation is seen between either class of stars and the ionized gas features: this may indicate that the region is rapidly loosing memory of the star formation process once the most massive stars,

say,  $M > 20M_{\odot}$ , have evolved and died producing SNII explosions.

EDITOR: PLACE FIGURE 6 HERE.

From Figure 6c, which displays the distributions of the two classes of stars in one and the same plot, it is apparent that they are distributed in substantially different manners. To better quantify this statement, we have divided the field into 9 regions: a circle of  $20''$  radius around SN 1987A and 8 radial sectors, as shown in Figure 6d.

EDITOR: PLACE TABLE 2 HERE.

Table 2 summarizes the areas of the 9 regions (note that for each sector the area reported in Table 2 corresponds to the area for which *both* broad band *and*  $H\alpha$  observations are available) their star number counts and the corresponding star densities per unit area. An inspection to this table reveals that there are enormous variations in the proportion of massive stars relative to low mass stars: in particular, the numbers of massive and low mass stars in the central area are almost the same, while in other areas the low mass stars are 7 to 28 times more numerous than massive stars. These differences are highly significant because they greatly exceed the expected Poissonian fluctuations, also given in Table 2. An experimental check of this fact is provided by similar statistics on the number of stars belonging to the so-called Red Giant Clump, *i.e.* stars of a much older population which, therefore, are expected to be uniformly distributed over the field. And indeed, as seen in Table 2, the observed number densities for Red Giant Clump stars show fluctuations which are perfectly compatible with Poisson statistics.

Another point worth noting is that the average density of T Tau stars in sectors 2+3 (*i.e.* East of SN 1987A) is  $(12.9 \pm 1.4)$ , *i.e.*  $3.5\sigma$  lower than the average  $18.6 \pm 0.8$ , whereas

in sectors 4+5 (South of SN 1987A) is  $3.9\sigma$  higher ( $27.4 \pm 2.1$ ). It would be tempting to interpret such a systematic difference in terms of a star formation “wave” or “front” that sweeps region. On the other hand, we do not find any significant difference in ages among PMS stars in the various sectors, suggesting that, rather than dealing with some sort of propagating star formation, the key factor here is the overall efficiency of the star formation process that varies from place to place. Also, we note that there is no enhancement in the density of T Tau stars around the SN 1987A cluster, nor near the brightest star in the observed field (see Figure 6c) lending support to the idea that the process of formation of low mass stars may be distinct from the one leading to the formation of massive stars.

## 6. SN 1987A Stellar Group: a “Typical” Cluster?

In Section 4 we have argued that massive stars are strongly concentrated around SN 1987A. This is clearly seen in Figure 7a (see also Fig. 1) that shows an area of about  $50'' \times 50''$  around SN 1987A: 14 stars brighter than  $10^3 L/L_\odot$  are found in the vicinities of the supernova. Actually, SN 1987A and its companions, Star 2 and Star 3, are at the Eastern edge of the stellar group, whose center almost coincides with a compact “core” of 8 blue stars. We note that the size of this stellar group associated with SN 1987A (about 9 pc) is similar to the average size of stellar clusters in the LMC ( $7.7 \pm 1.5$  pc; Hodge 1988) suggesting that we are dealing with a “canonical” LMC cluster. And, indeed, this group has been classified as a “loose cluster” by Kontizas *et al.* (1988; their No. 80).

EDITOR: PLACE FIGURE 7 HERE.

Walborn *et al.* (1993) discussed the properties of the cluster stars brighter than  $V \simeq 20$ . Analyzing their ground based  $UBV$  photometry, and adopting an average reddening of  $E(B-V) = 0.18$ , they concluded that the cluster had an age of about  $12 \pm 4$  million years.

As clearly seen in Figure 7b, with our data we can reduce the uncertainty and assign an age of  $12 \pm 2$  Myrs to the bulk of the stars present in this field. This age can fairly well account for the positions in the HR diagram of both the most massive stars (with one exception; see below) *and* the PMS stars found in this field. There is one bright star ( $\log T_{eff} \simeq 4.59$ ,  $\log L/L_{\odot} \simeq 4.51$ ) that appears to lie on the ZAMS and, therefore, to have a much younger age, say, 5 Myrs or less. While statistical errors cannot account for this discrepancy, we notice that this star displays a significant H $\alpha$  excess ( $W_{eq} \simeq 12\text{\AA}$ ) and, therefore, it is one of the 4 Be stars we mentioned in section 4. We argue that the strong Be characteristics are enough to alter the photospheric properties of this star so as to make it *appear* hotter and brighter than its average parameters would allow. In particular, if this is an almost pole-on Be star, we should *expect* its color temperature to be significantly higher than average. A “natural” consequence, which suggest a simple test to run, is that for a pole-on Be star the width of the H $\alpha$  emission is expected to be relatively narrow.

Given the number of stars in the mass range  $6\text{--}20 M_{\odot}$  (15 stars including the supernova progenitor), and adopting an IMF with slope  $\Gamma$  in the range -1 to -2, we estimate that the cluster originally included additional  $2 \pm 1$  stars in the mass range  $20\text{--}80 M_{\odot}$ , which exploded as SNII well before the SN 1987A event. However, there is no clear sign of any shell-like structure centered on the cluster. This implies that either the upper mass cutoff for *this* cluster was much lower than normal, *i.e.* no star more massive than  $\sim 20 M_{\odot}$  formed in this cluster, or the more massive stars gave origin to explosions involving considerably lower kinetic energies than the “canonical” value of  $10^{51} \text{ erg}$ .

The supernova is not at the center of the cluster but rather it is offset about  $15''$  to the East relative to the massive star barycenter, (*i.e.* the center of mass of 14 stars more massive than  $6M_{\odot}$  plus Sk -69 202 itself). We speculate that this lack of “prominence” for the supernova progenitor may indicate that the few cluster stars, which were more massive

than the SN 1987A progenitor and exploded long ago, were distributed over the cluster body, so as to fill the “gaps” between either the SN-Star2-Star3 group, or the SE cluster extension (4 massive stars), and the cluster center (8 massive stars).

## 7. Initial Mass Function: A Discussion

As pointed out in Section 5, the number ratio of PMS low mass ( $1-2 M_{\odot}$ ) stars to massive stars in the central cluster is much smaller than the average in the whole field, *i.e.* 1.4 as compared to the average value 8.9, indicating that there is an objective deficiency of low mass stars in this young cluster. Such a deficiency would translate into an IMF slope that over the approximate mass range  $1 - 14 M_{\odot}$  is considerably flatter than in the general field. In particular, if one adopts a slope  $\Gamma = d\log N / d\log M \simeq -1.5$  for the entire field (see next Section) the slope in the compact cluster would be approximately  $\Gamma = -0.5$ . On the other hand, a different conclusion would be reached if one limits the analysis to relatively high mass stars. For example, if one assumes all stars brighter than  $100L/L_{\odot}$  to belong to one and the same stellar generation, the IMF between  $3$  and  $14 M_{\odot}$  would turn out to have a slope  $\Gamma \simeq -1.2$ , *i.e.* very similar to Salpeter’s IMF. From these results one might conclude that a single power-law cannot represent the observations, and that the IMF agrees with Salpeter’s for masses higher than  $3M_{\odot}$  and flattens dramatically for lower masses.

On the other hand, it is rather incautious to talk about an IMF when dealing with small number statistics, and/or with very limited regions in space. In addition, looking at the cluster HR diagram (*c.f.* Fig. 7b) one can notice that many PMS stars appear to be appreciably older than 10 Myrs, and actually appear to cluster around a 20 Myrs isochrone. This fact, while confirming that the most recent stellar generation is poor of low mass stars, also tells us that the formation of lower mass stars in the cluster region is occurring on different timescales than that of more massive stars.

On a larger scale, the almost anti-correlation of the spatial distributions of high mass and low mass stars of a coeval generation (*c.f.* Section 5, and Fig. 6) indicates that star formation processes for different ranges of stellar masses are rather different and/or require different initial conditions. An important corollary of this result is that the very concept of an “initial mass function” (IMF) may not have validity in detail, but rather be the result of a chaotic process, so that it may make sense to talk about an *average IMF* over a suitably large area in which all different star formation processes are concurrently operating. Actually, if we just take the ratio of the total numbers of massive to low-mass stars belonging to the young population as reported in Table 2, and interpret them in terms of a power-law IMF adopting mass intervals of  $6-15 M_{\odot}$  and  $1-2 M_{\odot}$  for massive stars and for PMS stars, respectively, we would derive a slope of the initial mass function of  $\Gamma = d\log N / d\log M \simeq -1.3$  with a purely statistical uncertainty of  $\pm 0.1$ . Such a value is remarkably close to the classical Salpeter’s (1955) slope  $\Gamma = -1.35$  for the Solar neighborhood and is valid over essentially the same mass interval as the original Salpeter’s analysis, *i.e.*  $\sim 2-10 M_{\odot}$ . However, this is a conclusion drawn without taking into account of possible incompleteness effects. On the one hand, for both massive and low mass stars above  $\sim 1 M_{\odot}$ , incompleteness due to missed detection and/or to crowding/blending is a negligible effect because all of these stars are well above our detection limit and their surface density is not so high (1 star per  $\sim 170$  WF pixel area, or, equivalently, an average separation of stars of  $\sim 13$  WF pixels). On the other hand, for PMS stars one has to bear in mind that we can reliably identify only strong-line T Tau stars and that the *total* number of PMS stars of comparable masses may be considerably larger. For example, Alcalá *et al.* (1996) have shown that in the Orion region the number of weak-line T Tau stars is at least comparable to, and possibly larger than that of strong-line T Tauri stars. Actually, if one would identify PMS stars on the basis of their UV excess, *i.e.* as stars with much bluer  $U - B$  colors than expected for normal stars with their observed  $B - V$  and  $V - I$  colors,

one would count in our field as many as  $\sim 850$  PMS stars (Romaniello 1998), *i.e.* a factor of 1.7 more than the positively identified T Tau stars. Moreover, T Tau stars are known to exhibit strong H $\alpha$  variability on short timescales (*e.g.* Smith et al. 1999, and references therein). As a consequence, at any one time one may be able to detect only a fraction of the entire population of strong-line T Tau stars. Indeed, preliminary comparisons of overlapping regions in fields imaged at two different epochs (about 15% of the entire field around SN 1987A) have shown that, while the number of strong-line T Tau stars identified at any one time is essentially constant, no more than half of the candidate T Tau stars display a significantly strong H $\alpha$  excess at both epochs (Romaniello and Panagia 1999). This suggests that the total number of PMS stars may easily be twice as high as the number of strong-line T Tau stars we have identified, and possibly even higher. In turn, this result implies a significantly steeper IMF slope, say,  $\Gamma \simeq -1.7$  or even more negative. A detailed discussion of these effects is presented in Romaniello (1998). Eventually, combining observations of the SN 1987A field taken at substantially more epochs than available at present, we will be able to properly identify *all* T Tau stars in the field so as to obtain a reliable statistics of the young population in the neighborhood of SN 1987A and to reach firm conclusions about star formation processes and history in this region of the LMC (Romaniello and Panagia 1999).

It is important to realize how crucial it is to *individually* identify and characterize each and everyone of the PMS stars if one wants to evaluate an IMF reliably. For example, in our field we can identify about 500 PMS stars using an H $\alpha$  excess criterion, and possibly almost 1000 on the basis of a UV excess. Still, such numbers represent a small fraction of the *total* number of stars with temperatures and luminosities comparable to those of the candidate PMS stars. Actually, limiting ourselves to stars which in the HR diagram fall between the 5 and 40 *Myrs* PMS isochrones and which are brighter than  $L_\odot$  (*i.e.* for stars whose statistics is pretty complete), the ratio of the total number of stars to the number

of *bona fide* PMS stars is  $\sim 20$  if we include all possible candidates, and more than 40 if we include only strong-line T Tau stars. This means that in the absence of an explicit characterization of PMS stars, using just the location of stars in the HR diagram as the criterion to recognize PMS stars will unavoidably introduce some heavy contamination. One can argue that, for a fixed surface density of old population stars, such an effect is much reduced when studying regions containing large concentrations of young stars. For instance, the possible contamination by older populations could be, say, 10% or less, if the surface density of young stars in a given region were higher than 200-400 times the density of young stars around SN 1987A or, equivalently, 10 times the density of old population stars in the SN 1987A vicinities. However, since the density of old population stars with luminosities in the range  $1 < L/L_\odot < 10$  is about 0.2 stars per square arcsecond, exceeding that density by a factor of 10, at least, would imply an average density of young population, low mass stars ( $1 < L/L_\odot < 10$ ) higher than 2 stars per square arcsecond, and at least ten times higher for stars in the next 1-*dex* bin in luminosity. It is easy to realize that with such high stellar densities another problem is bound to arise, at least for low mass stars, namely confusion/blending due to crowding. These effects will both “drown” faint stars into a “sea” of even fainter stars and/or would artificially create brighter stars by confusing nearby stars into one more luminous, apparently point-like source (Panagia 2000).

From this discussion, it follows that it is essential to have *spectroscopic* criteria that allow one to discern PMS stars from field stars unambiguously and completely. H $\alpha$  excess and/or UV excess are possible ways of accomplishing this goal, but even these methods need confirmation, calibration and sharpening, in that we still have to compare our multi-band photometry (or “wide-band spectroscopy”) with *real* spectra before a 100% reliable of identification of T Tau stars can be claimed. We are going to fill this gap by taking medium-high resolution spectra of a number of our best T Tau candidates with the ESO-VLT1 in January 2000 (Favata et al. 2000). With that it will eventually be possible

to start talking about low mass star formation and low end of the IMF in the LMC on firm scientific grounds.

## 8. Conclusions

We have analyzed the *WFPC2* images obtained in the UV, U, B, V, R, I broad bands, plus the [OIII] and H $\alpha$  narrow band filters, of the 130'' radius region centered on SN 1987A, focusing on the properties of the stellar populations present in the field. The main results can be summarized as follows:

- Over the entire field, we identify 21,995 stars, of which 5,979 have an overall photometric accuracy in the optical bands better than 0.1*mag*.
- From a comparison of the available 6 broad band photometry with model atmospheres, we have determined effective temperatures and bolometric luminosities for all of the 21,995 stars. For a subset of 2,510 we also determined individual reddening corrections. Overall, we obtained an excellent characterization of a large fraction of the sample stars. In particular, the effective temperature was determined with an uncertainty lower than 0.05 *dex* in  $\log(T_{eff})$  for 9,474 stars, most of which are brighter than  $L/L_{\odot}=1$ .
- From an analysis of the resulting HR diagram we have found evidence for a series of star formation episodes spanning from several billion years ago until at least 1-2 *Myrs* and, possibly, still ongoing.
- We have identified a generation of stars with ages about 10-12 *Myrs* which is coeval to the supernova progenitor and may include up to 35% of the young population in the entire field (defined as stars with ages < 100 *Myrs*).

- The properties of the field old population indicates strong and continued star formation over a broad interval of  $0.6 - 6$  *Gyrs*.
- We have identified 488 strong-line *T Tauri* stars on the basis of their conspicuous ( $W_{eq} > 8\text{\AA}$ )  $\text{H}\alpha$  excesses. Their ages peak at about 10-20 *Myrs* and range from about 1 *Myrs* up to possibly 40 *Myrs*. Their positions in the HR diagram appear to require that star formation in the LMC occurs with accretion rates about 10 times higher than in the Milky Way, *i.e.*  $\sim 10^{-4}M_{\odot} \text{ yr}^{-1}$ . This constitute the first positive detection of low mass (about  $1-2 M_{\odot}$ ) PMS stars outside the Milky Way.
- SN 1987A appears to belong to a loose, young cluster  $12 \pm 2$  *Myrs* old, in which the slope of the present mass function is almost identical to Salpeter's, *i.e.*  $\Gamma \simeq -1.25$  for masses above  $3 M_{\odot}$ , but becomes much flatter for lower masses, *i.e.*  $\Gamma \simeq -0.5$ .
- A comparison of the spatial distributions of massive stars and low-mass PMS stars shows that they are conclusively different, which indicate that different star formation processes operate for high and low mass stars.
- We have addressed the problem of determining an IMF in our field. Because of the substantial differences of the spatial distributions of stars of different masses in our field, we conclude that the very concept of an IMF is not valid on a small scale (say,  $< 10 \text{ pc}$  diameter, *i.e.* a scale comparable to the size of SN 1987A cluster) but it may become meaningful on a larger scale. A preliminary analysis shows that, averaging over the whole region (about  $60\text{pc}$  diameter), the IMF slope is steeper than Salpeter's IMF, *i.e.*  $\Gamma \simeq -1.7$ .
- Since even the young stellar population is a mixture of generations of stars with different ages, we have concluded that a study of the IMF requires a proper separation of *all* of the various stellar populations coexisting with each other. We have shown

that a proper characterization of the low mass end of the IMF requires explicit identification of individual PMS stars.

SS acknowledge the kind hospitality of STScI, where most of this work was done, as well as partial support from the STScI Visiting Scientist Program. The comments of an anonymous referee were valuable to improve the presentation. This work was supported in part by HST-STScI grants GO-6437, GO-7434 GO-7821, GO-8243 to the SINS project (PI: RPK) and by STScI-DDRF grants # 82131, 82160, and 82186 to NP.

Table 1: Log of the observations centered on Supernova 1987A.

Filter Name	Exposure Time (seconds)			Comments
	September 1994 <sup>a</sup>	February 1996 <sup>b</sup>	July 1997 <sup>c</sup>	
<b>F255W</b>	2x900	1100+1400	2x1300	UV Filter
<b>F336W</b>	2x600	2x600	2x800	U Filter
<b>F439W</b>	2x400	350+600	2x400	B Filter
<b>F555W</b>	2x300	2x300	2x300	V Filter
<b>F675W</b>	2x300	2x300	2x300	R Filter
<b>F814W</b>	2x300	2x300	2x400	I Filter
<b>F502N</b>	4x1200	1100+1500	2x1300+4x1400	[OIII] $\lambda$ 5007 Å
<b>F656N</b>	—	1100+1300 <sup>d</sup>	4x1400	H $\alpha$
<b>F658N</b>	4x1200	1100+1500	—	[NII] $\lambda$ 6584 Å <sup>e</sup>

<sup>a</sup>September 24, 1994, proposal number 5753.

<sup>b</sup>February 6, 1996, proposal number 6020.

<sup>c</sup>July 10, 1997, except for F502N taken on July 12, 1997, proposal number 6437.

<sup>d</sup>Not from SINS (PI John Trauger), taken on February 3, 1994.

<sup>e</sup>With  $\sim$ 25% H $\alpha$  contamination.

Table 2: **Spatial distribution of stars around SN1987A** - Observed numbers and derived densities of the various types of stars in the regions illustrated in Figure 4d. The quoted errors are the expected fluctuations according to Poisson statistics.

Region	Area <sup>a</sup>	Massive stars <sup>b</sup>		T Tauri stars <sup>c</sup>		Red Giants <sup>d</sup>		
		Number	Density	Number	Density	Number	Density	
C	1.00	14	$14 \pm 3.7$	20	$20.0 \pm 4.5$	16	$16.0 \pm 4.0$	
1	4.70	10	$2.1 \pm 0.7$	81	$17.2 \pm 1.9$	62	$13.2 \pm 1.7$	
2	3.80	9	$2.4 \pm 0.8$	50	$13.2 \pm 1.9$	48	$12.6 \pm 1.8$	
3	3.16	6	$1.9 \pm 0.8$	40	$12.6 \pm 2.0$	34	$10.7 \pm 1.8$	
4	3.02	6	$2.0 \pm 0.8$	83	$27.5 \pm 3.0$	40	$13.2 \pm 2.1$	
5	3.14	3	$1.0 \pm 0.6$	84	$26.8 \pm 2.9$	57	$18.2 \pm 2.4$	
6	2.31	0	0	38	$16.4 \pm 2.7$	37	$16.0 \pm 2.6$	
7	2.41	3	$1.2 \pm 0.7$	43	$17.8 \pm 2.7$	38	$15.8 \pm 2.6$	
8	2.69	4	$1.5 \pm 0.7$	49	$18.2 \pm 2.6$	25	$9.3 \pm 1.9$	
Total		26.23	55	$2.1 \pm 0.3$	488	$18.6 \pm 0.8$	357	$13.6 \pm 0.7$

<sup>a</sup>In units of the area of the central cluster ( $20''$  radius, *i.e.* 1207 square arcseconds).

<sup>b</sup> $\log(L/L_{\odot}) > 3$ ,  $M > 6 M_{\odot}$ .

<sup>c</sup> $EW(H\alpha) \gtrsim 8 \text{ \AA}$ ,  $1 M_{\odot} < M < 2 M_{\odot}$ .

<sup>d</sup> $3.65 < \log(T_{\text{eff}}) < 3.9$  and  $1.5 < \log L/L_{\odot} < 2.1$ , LMC field population.

## REFERENCES

Alcalá, J.M., et al., 1996, A&AS, 119, 7.

Bessel, M.S., Castelli, F., and Plez, B. 1998, A&A, 333, 231; erratum A&A, 337, 321.

Biretta, J.A., 1996, *WFPC2* Instrument Handbook 4.0, Space Telescope Science Institute, Baltimore.

Brocato, E., and Castellani, V. 1993, ApJ, 410, 99.

Burrows, C.J. et al 1995, ApJ, 452, 680.

Cassisi, S., Castellani, V., and Straniero, O. 1994, A&A, 282, 753.

Frasca, A., and Catalano, S. 1994, A&A, 284, 883.

Favata, F., Romaniello, M., Gilmozzi, R., Panagia, N., and Scuderi, S., 2000, in preparation.

Fernandez, M., Ortiz, E., Eiroa, C., and Miranda, L.F., 1995, A&AS, 114, 439.

Gilliland, R.L., 1994, ApJ, 435, L63.

Gilmozzi, R. 1990, “Core aperture photometry with the WFPC”, STScI Instrument Report WFPC-90-96.

Gilmozzi, R., Kinney, E.K., Ewald, S.P., Panagia, N., and Romaniello, M., 1994, ApJ, 435, L45.

Herbig, G.H., 1960, ApJS, 4, 337.

Herbig, G.H., & Bell, K.R., 1988, *Lick Obs. Bull.* No. 1111.

Hodge, P.W. 1988, PASP, 100, 1051.

Hunter, D.A., Shaya, E.J., Holtzman, J.A., Light, R.M., O'Neill, E.J., & Lynds, R., 1995, ApJ, 448, 179.

Jakobsen, P., et al. 1991, ApJ, 369, L63.

Jaschek, M., Hubert-Delplace, A.M., Hubert, H., & Jaschek, C., 1980, A&AS, 42, 103.

Lamers, H.J.G.L.M., Beaulieu, J.P., and de Wit, W.J., 1999, A&A, 341, 827.

Lucke, P.B., and Hodge, P.W. 1970, AJ, 75, 171.

Kontizas, E., Metaxa, M., & Kontizas, M., 1988, AJ, 96, 1625.

Palla, F., & Stahler, S.W., 1993, ApJ, 418, 414.

Panagia, N., Gilmozzi, R., Macchetto, F.D., Adorf, H.-M., and Kirshner, R. P. 1991, ApJ, 380, L23.

Panagia, N., Scuderi, S., Gilmozzi, R., Challis, P. M., Garnavich, P. M., and Kirshner, R. P. 1996, ApJ, 459, L17.

Panagia, N. 1999, in IAU Symposium #190 *New Views of the Magellanic Clouds*, eds. Y.-H. Chu, N. Suntzeff, J. Hesser, & D. Bohlender, Astr. Soc. Pacific (San Francisco, Calif.), p. 549-556.

Panagia, N., Gilmozzi, R., Kirshner, R.P., Pun, J.S., and Sonneborn, G. 1999, ApJ, to be submitted.

Panagia, N., 2000, in preparation.

Romaniello, M. 1998, PhD Thesis, Scuola Normale Superiore, Pisa, Italy.

Romaniello, M., and Panagia, N. 1999, in preparation

Romaniello, M., Panagia, N., Scuderi, S., and Kirshner, R.P. 1999a, in preparation.

Romaniello, M., Salaris, M., Cassisi, S., and Panagia, N., 1999b, ApJ, in press  
[astro-ph/9910082].

Salpeter, E. 1955, ApJ, 121, 161.

Scuderi, S., Panagia, N., Gilmozzi, R., Challis, P.M. and Kirshner, R.P. 1996, ApJ, 465,  
956.

Siess, L., Forestini, M., and Dougados, C. 1997, A&A, 324, 556.

Smith, K.W., Lewis, G.F., Bonnel, I.A., Bunclark, P.S., and Emerson, J.P., 1999, MNRAS,  
304, 367.

Suntzeff, N. 1998, Proc. ESO/CTIO/LCO Workshop *SN 1987A: Ten Years After*, eds. M.  
Phillips and N.B. Suntzeff, A.S.P. Conf. Ser., in press.

Van Dyk, S., Hamuy, M., and Mateo, M. 1998, Proc. ESO/CTIO/LCO Workshop  
*SN 1987A: Ten Years After*, eds. M. Phillips and N.B. Suntzeff, A.S.P. Conf. Ser., in  
press.

Walborn, N.R., Philips, M.M., Walker, A.R., and Elias, J.H. 1993, PASP, 105, 1240.

Walker, A.R., and Suntzeff, N.B. 1990, PASP, 102, 131.

Whitmore, B., 1995, in *Calibrating Hubble Space Telescope: Post Servicing Mission*, ed. A.  
Koratkar and C. Leitherer, Space Telescope Science Institute, p.269.

Fig. 1.— The field centered on SN1987A (about  $130''$  radius) as observed in the combination of the B, V, and I broad bands plus the [OIII] and H $\alpha$  narrow band images. The blue, bright star about  $94''$  NE of SN 1987A is the brightest ( $\log(L/L_\odot) \simeq 5.8$ ) and most massive ( $\sim 60M_\odot$ ) star in the field (see Sections 4 and 5).

Fig. 2.— Color-Magnitude Diagrams for four combination of filters. The grey dots are stars with average errors (as defined in Eq. (1))  $\bar{\delta}_5 > 0.1$ , whereas the black dots are the 5,979 stars with  $\bar{\delta}_5 < 0.1$ .

Fig. 3.— The HR diagram for the stars in the *WFPC2* field. The grey dots are stars with average errors (as defined in Eq. (1))  $\bar{\delta}_5 > 0.1$ , whereas the black dots are the 6695 stars with  $\bar{\delta}_5 < 0.1$ . [a] (left panel): Comparison with the theoretical ZAMS for different Z values:  $Z = Z_\odot$  long dashed line,  $Z = 0.3Z_\odot$  solid line, and  $Z = Z_\odot/20$  dotted line. [b] (right panel): Comparison with a number of post-MS isochrones (Brocato and Castellani 1993, Cassisi *et al.* 1994). The brightest star in the field, possibly a  $\sim 60M_\odot$  star younger than 1 *Myrs*, is marked with a circle at the top of the diagram.

Fig. 4.— The HR diagram displaying the positions of the stars with strong H $\alpha$  excess (dots) overlayed on the general stellar population (grey squares) found in the *WFPC2* field. For reference, we show the theoretical ZAMS (Brocato and Castellani 1993) with marked position for stars of various masses. Also shown are 2.5-20 *Myrs* PMS isochrones (Siess *et al.* 1997) and the birthlines for accretion rates of  $10^{-4}$  (short-dashed line) and  $10^{-5} M_\odot \text{ yr}^{-1}$  (long-dashed line; Palla & Stahler 1993).

Fig. 5.— The distribution of number of stars with strong H $\alpha$  emission per unit of 0.2 *dex* bin of the H $\alpha$  equivalent width,  $W_{eq}(H\alpha)$ . Candidate Be stars have been excluded from this histogram. The shaded histogram is the corresponding distribution for galactic strong-line T Tau stars (Fernandez *et al.* 1995).

Fig. 6.— Comparison of the spatial distributions of massive stars ( $M > 6M_{\odot}$ , star symbols) and PMS stars ( $M < 2M_{\odot}$ , squares) belonging to the same younger population. North is up and East is to the left. [a] (*upper left*): Massive stars overlayed on a mosaic of *WFPC2* H $\alpha$  images. [b] (*upper right*): PMS stars overlayed on a mosaic of *WFPC2* H $\alpha$  images. [c] (*lower left*): Massive stars (blue star symbols) and PMS stars (red square symbols) overlayed on the general field including 21,995 stars (little dots). The brightest star ( $\log(L/L_{\odot}) \simeq 5.8$ ) is denoted with a larger size, pale blue star symbol. [d] (*lower right*): Number of massive stars (blue), PMS stars (red) and Red Giant Clump stars (black) in a central circle centered on SN 1987A and in 8 sectors (*c.f.* Table and Section 5).

Fig. 7.— The properties of the central cluster: *Left panel* - The combined BVR plus H $\alpha$  image of an area  $50'' \times 50''$  around SN 1987A. *Right panel* - The corresponding HR diagram in which stars with strong H $\alpha$  excess are denoted with red symbols. Isochrones for post-MS evolution at 10 and 14 Myrs, and PMS evolution at 5, 10 and 20 Myrs are also shown.

This figure "Fig1.gif" is available in "gif" format from:

<http://arxiv.org/ps/astro-ph/0001476v1>

This figure "Fig2.gif" is available in "gif" format from:

<http://arxiv.org/ps/astro-ph/0001476v1>

This figure "Fig3a.gif" is available in "gif" format from:

<http://arxiv.org/ps/astro-ph/0001476v1>

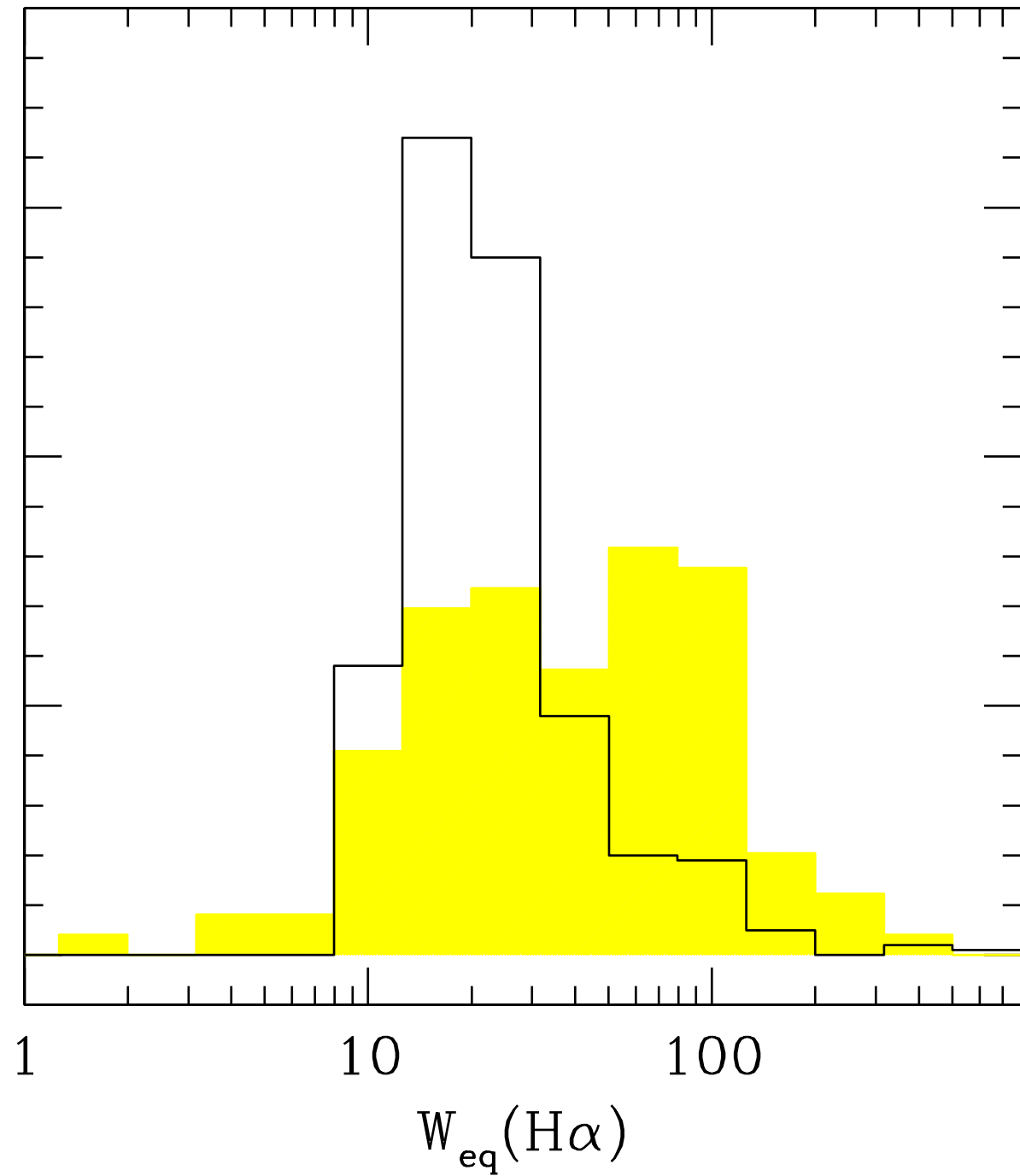
This figure "Fig3b.gif" is available in "gif" format from:

<http://arxiv.org/ps/astro-ph/0001476v1>

This figure "Fig4.gif" is available in "gif" format from:

<http://arxiv.org/ps/astro-ph/0001476v1>

number of stars per 0.2 dex bin

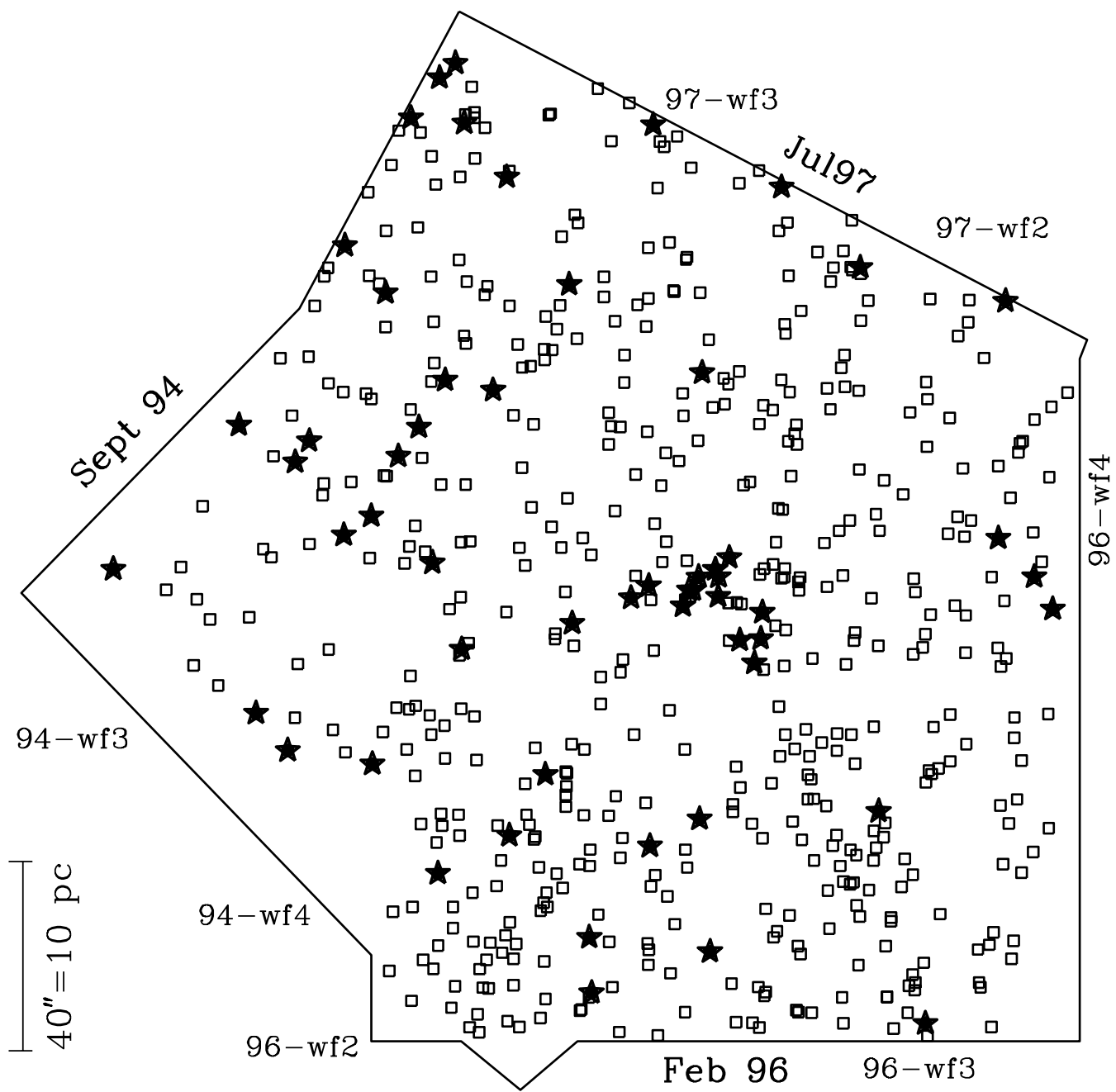


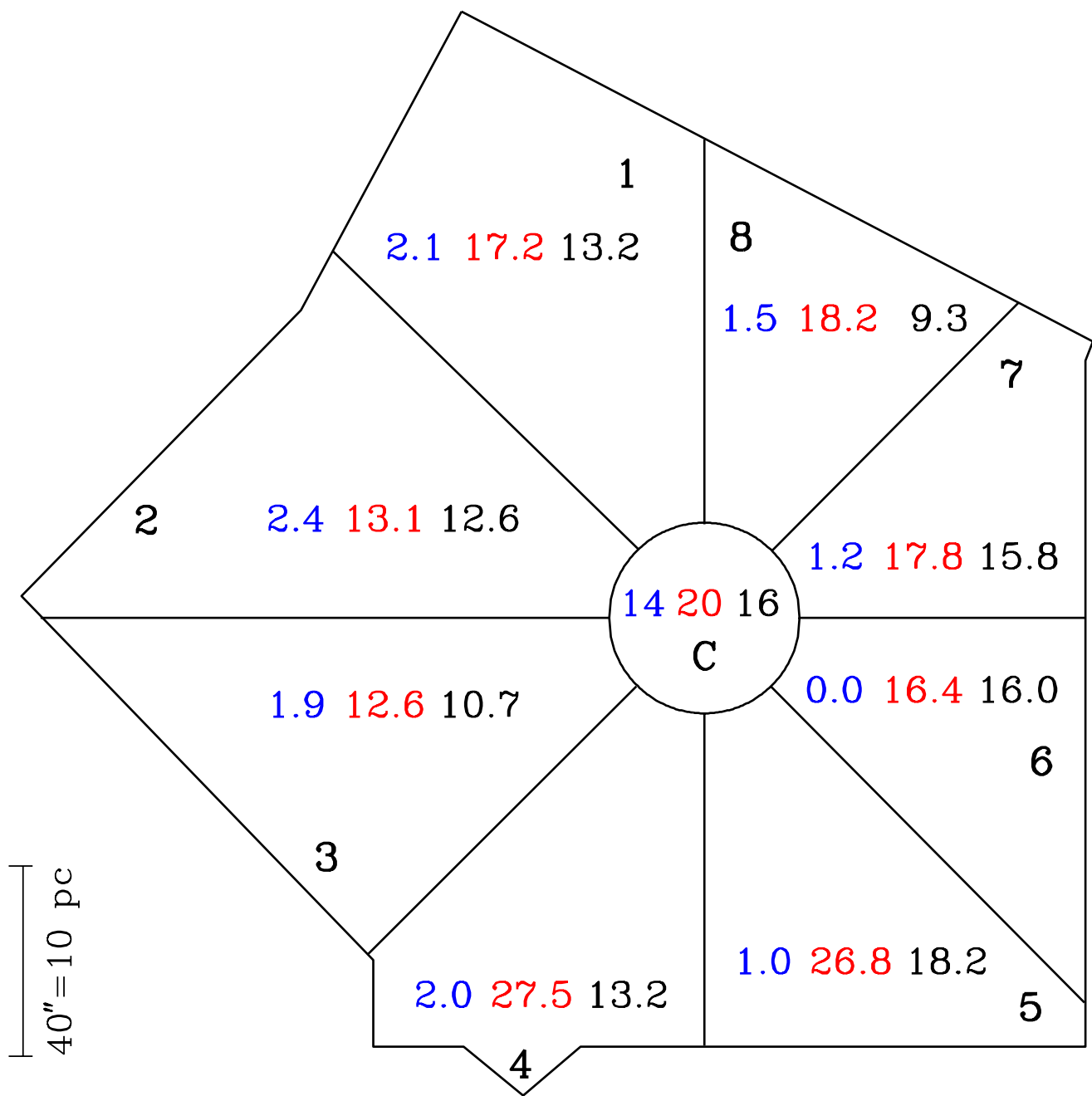
This figure "Fig6a.gif" is available in "gif" format from:

<http://arxiv.org/ps/astro-ph/0001476v1>

This figure "Fig6b.gif" is available in "gif" format from:

<http://arxiv.org/ps/astro-ph/0001476v1>





This figure "Fig7a.gif" is available in "gif" format from:

<http://arxiv.org/ps/astro-ph/0001476v1>

This figure "Fig7b.gif" is available in "gif" format from:

<http://arxiv.org/ps/astro-ph/0001476v1>